UNIVERSITY OF CALIFORNIA
RIVERSIDE

# Function of TPPI and TPPJ in *Arabidopsis* Boundary Regions

A Thesis submitted in partial satisfaction
of the requirements for the degree of

Master of Science

in

Plant Biology

by

Jessica Lynn Lor

December 2014

Thesis Committee:
Dr. Patricia Springer, Chairperson
Dr. Linda Walling
Dr. Venu Reddy

The Thesis of Jessica Lynn Lor is approved:

_____

_____

_____

Committee Chairperson

University of California, Riverside

**Acknowledgments**

I would first like to thank my advisor, Dr. Patricia Springer, for guiding me through this entire journey. Even simple tasks seemed like a struggle at times, but she was always willing to help me persevere. I sincerely appreciate her taking time to discuss my work, teach me new techniques, proofread my papers and help me grow as a scientist. The skills I have developed from her during my time here will always be of value.

I would also like to thank both of my committee members, Dr. Linda Walling and Dr. Venu Reddy. They have both provided me with words of encouragement and have taken the time to give advice towards my progress. Dr. Reddy allowed me to develop new skills in his lab and Dr. Walling was always there to listen to my struggles without judgment.

I am very grateful to have worked with all the members in the Springer Lab, who were always there for me. Each member took time to teach me new techniques and made lab a positive environment. They have made my time here enjoyable and have become lifelong friends. Special thanks are given to Barbara Jablonska and Robert Koble for providing assistance with this work.

Finally, I would like to thank my family for always believing in me and providing nonstop support. My husband, Kao Lor, deserves the greatest thank you because he was here for me every step of this journey. He made the move to CA with me, stayed up many late nights with me and kept me sane by being my emotional support.

ABSTACT OF THE THESIS

Function of TPPI and TPPJ in *Arabidopsis* Boundary Regions

by

Jessica Lynn Lor

Master of Science, Graduate Program in Plant Biology
University of California, Riverside, December 2014
Dr. Patricia Springer, Chairperson

The shoot apical meristem (SAM) located at the shoot tip of a plant, produces all above ground organs including leaves and flowers. Separating the SAM and a lateral organ is the boundary region, which has distinctive cellular properties. The boundary region has many important functions including organ separation and axillary meristem formation. It is known that *LATERAL ORGAN BOUNDARIES* (*LOB*), an organ boundary gene, plays a role in organ separation by limiting growth in the boundary region. Through microarray and qRT-PCR, a *TREHALOSE PHOSPHATE PHOSPHATASE* gene, *TPPJ*, has been identified as a potential downstream target of LOB. Trehalose phosphate phosphatases (TPPs) are known to regulate the production of metabolic intermediates of the trehalose biosynthesis pathway in plants. The overall objective of this research was to investigate the function of *TPPJ* and its paralog, *TPPI,* in the boundary region of *Arabidopsis*. The first goal was to characterize *TPPI* and *TPPJ* loss-of-function mutants in order to determine if these

genes have a function in the boundary region. The second goal was to characterize the genetic relationship between *LOB* and *TPPI* and *TPPJ* using genetic and transgenic approaches. It was discovered that the *tppj-sk* T-DNA insertion line has reduced levels of *TPPJ* transcript. Furthermore, expression of *TPPJ* in the boundary under control of the *LOB* promoter (*pLOB:TPPJ)* suppressed organ fusion in the *lob-3* mutant, showing *TPPJ* is sufficient to rescue the *lob* mutant phenotype. *tppi-1* loss-of-function mutants displayed a decurrent strand fusion phenotype, indicating that *TPPI* also has a role in organ separation. In addition, *tppi-1* mutants were late flowering, indicating that *TPPI* may also be involved in the transition from vegetative to reproductive development. Together, this work provides a starting point for determining the function of *TPPI* and *TPPJ* in the boundary region of *Arabidopsis*.

TABLE OF CONTENTS

Acknowledgements iv

Abstract v

Table of Contents vii

List of Figures viii

Introduction 1

Results 14

Discussion 22

Materials and Methods 26

References 30

Figures 37

Tables 50

LIST OF FIGURES

FIGURE 1 STRUCTURE OF THE *TPPJ-SK* T-DNA ALLELE (sk476)_____37

FIGURE 2 *TPPJ* TRANSCRIPT LEVELS IN DISSECTED INFLORESCENCES AND PARACLADE JUNCTIONS _____38

FIGURE 3 EXPRESSION OF *TPPJ* UNDER THE *LOB* PROMOTER SUPRESSES FUSION IN THE *lob* MUTANT_____39

FIGURE 4 *pLOB:TPPJ* RESCUES *LOB-3* FUSION PHENOTYPE_____40

FIGURE 5 STRUCTURE OF THE *TPPI-1* T-DNA ALLELE (SAIL_354_D09)_____41

FIGURE 6 PRESENCE OF DECURRENT STRAND IN *TPPI*-1 MUTANTS _____42

FIGURE 7 LENGTH OF CONTACT BETWEEN AXILLARY STEM AND CAULINE LEAF IS SIMILAR BETWEEEN t*ppi-1* MUTANTS AND *TPPI/TPPI* _____43

FIGURE 8 DECURRENT STRANDS OCCUR MOST FREQUENTLY IN *tppi-1* MUTANTS COMPARED TO TPPI/TPPI _____44

FIGURE 9 LENGTH OF DECURRENT STRANDS IS INCREAESD IN t*ppi-1* MUTANTS COMPARED TO *TPPI/TPPI* _____45

FIGURE 10 DECURRENT STRAND AND ROUND ROSETTE LEAVES PRESENT IN *tppi-*1 and *lob-3 tppi-1* MUTANTS _____46

FIGURE 11 LENGTH OF CONTACT BETWEEN AXILLARY STEM AND CAULINE LEAF IN *lob-3* and *lob-3 tppi-1* MUTANTS _____47

FIGURE 12 LENGTH OF DECURRENT STRANDS IN *tppi-1* and *lob-3 tppi-1* MUTANTS _____48

FIGURE 13 *TPPI-1* MUTANTS SHOW DELAYED FLOWERING_____49

## Introduction

### Development and Function of the Boundary Region

All above ground organs including leaves and flowers are produced from the shoot apical meristem (SAM), which is located at the shoot apex of the plant. The SAM consists of a population of self-renewing stem cells located in the central zone, which divide to produce daughter cells in the peripheral zone. A subset of cells in the peripheral zone are incorporated into organ primordia to form new lateral organs (Szymkowiak and Sussex, 1996; Barton, 2010). Maintenance of a balance between the central stem cells and peripheral zone cells is necessary in order to preserve the SAM and lateral organ formation.

Separating the SAM and lateral organ is the boundary region, which has distinctive cellular properties. The boundary is composed of cells that are smaller and divide infrequently compared to neighboring cells that are actively dividing (Hussey, 1971; Breuil-Broyer et al., 2004; Rast and Simon, 2008). Hussey examined the surface of tomato apices and noticed that the boundary cells that had slower rates of division than neighboring cells (1971). Cell division in the *Arabidopsis* inflorescence apex was monitored by labeling with the nucleotide analog BrdU, which marks dividing cells (Breuil-Broyer et al., 2004). The authors observed bands of reduced cell division between the inflorescence meristem and floral meristems and between floral organ primordia and the floral meristem. The areas of reduced BrdU labeling correlated with the expression patterns of a boundary gene whereas

positive regulators of cell proliferation were only expressed in neighboring regions and were absent in the boundary (Breuil-Broyer et al., 2004).

Another distinguishing feature of boundary cells is that several genes have been shown to be specifically expressed in these cells (Rast and Simon, 2008). Genes expressed in the boundary region have been shown to play a role in organ separation, boundary formation and axillary meristem formation. These genes include *LATERAL ORGAN FUSION 1/2* (*LOF1/2), JAGGED LATERAL ORGANS (JLO)*, *CUP-SHAPED COTYLEDON1/2/3 (CUC1/2/3), LATERAL SUPPRESSOR (LAS), BLADE ON PETIOLE1/2 (BOP1/2)* and *REGULATOR OF AXILLARY MERISTEMS1/2/3 (RAX1/2/3)* (Borghi et al., 2007; Rast and Simon, 2012; Aida et al., 1997; Aida et al., 1999; Takada et al., 2001; Vroemen et al., 2003; Lee et al., 2009; Greb et al., 2003; Ha et al., 2003; Hepworth et al., 2005; Keller et al., 2006; Muller et al., 2006). *LOF1* and *LOF2* encode MYB transcription factors and function in organ separation and axillary meristem formation (Lee et al., 2009). JLO, a transcription factor, is expressed at the site of organ initiation and is required for the initiation of cotyledons (Borghi et al., 2007; Rast and Simon, 2012). *JLO* is also expressed in boundaries between meristems and organ primordia, where it plays a role in organ separation (Borghi et al., 2007). Dominant-negative transgenic plants expressing a fusion of JLO to the EAR transcriptional repression domain exhibit partially fused cotyledons and upward curled leaves (Borghi et al., 2007). *LAS,* which is expressed between the meristem and organ primordia, encodes a GRAS-family transcription factor (Greb et al., 2003). LAS activity is necessary for initiation of axillary

meristems (Greb et al., 2003). BOP1/2 both function in proximal-distal leaf patterning, floral symmetry and floral organ abscission (Hepworth et al., 2005). *RAX* genes encode MYB transcription factors and play a role in axillary meristem formation (Keller et al., 2006; Muller et al., 2006).

The multiple boundary-expressed genes are involved in three defining functions of the boundary region. The first function is to control organ separation by limiting growth within the boundary region (Hussey, 1971; Breuil-Broyer et al., 2004; Rast and Simon, 2008). *CUC* genes are expressed specifically in the boundary region and suggest boundary genes function in organ separation (Aida et al., 1997). Mutations in *CUC* genes result in fused cotyledons and fused floral organs such as sepals and stamens (Aida et al., 1997). The boundary region is also the site of abscission, the shedding of leaves, flowers and fruits, which involves a programmed cell death process (Jinn et al., 2000). HAESA, a receptor-like protein kinase, is expressed in organ boundaries at the base of sepals, petals, stamens, pedicels and petioles and plays a role in floral organ abscission (Jinn et al., 2000). Finally, organ boundaries are the site of axillary meristem formation, which form in the axils of leaves (Rast and Simon, 2008; Barton, 2010). Axillary meristems allow for the production of additional flowers and regulate the overall plant structure (Rast and Simon, 2008; Barton, 2010). Boundary genes involved in axillary meristem formation include *RAX*, *LOF1/2*, *LAS* and *CUC1/2/3* (Muller et al., 2006; Lee et al., 2009; Greb et al., 2003; Raman et al., 2008).

Identifying ways to increase crop yields has become a necessity as the world population continues to rise. By altering plant architecture, crop yields might be increased without requiring additional land for planting. Organ boundaries have a significant impact on plant architecture, as they are the sites at which features such as leaf angle and inflorescence branching are controlled (Rast and Simon, 2008). For example, in rice the boundary between the blade and sheath, the lamina joint, plays a significant role in determining leaf angle and the overall structure of the plant. Understanding the control of leaf angle might lead to the generation of plants with more erect leaf angles, allowing higher planting densities (Sakamoto et al, 2006). In fact, over the past century, breeding for an erect-leaf architecture in maize has resulted in increased yields due mostly to higher planting densities and not necessarily more yield per plant (Tian et al., 2011; Duvick, 2005). As maize leaves have become more erect, the average plant density has increased by 50,000 plants per hectare in the last eighty years (Tian et al., 2011; Duvick, 2005). It is beneficial to study the functions of boundary genes in *Arabidopsis*, because these findings can increase the understanding of shoot architecture regulation in staple crops.

## *LATERAL ORGAN BOUNDARIES* (*LOB*) Encodes a Transcription Factor in the Boundary Region

The LOB-domain family (LBD), a plant-specific gene family, consists of 43 members in *Arabidopsis* (Shuai et al., 2002). This family is divided into two classes based on their similarity to LOB, however all members of the LBD family contain the

LOB domain (Shuai et al., 2002). The LOB domain is approximately 100 amino acid residues and consists of a conserved DNA-binding motif (Shuai et al., 2002; Husbands et al., 2007). *LBD* genes encode DNA-binding transcription factors that recognize the LBD motif, a 6-bp consensus sequence 5′-(G)CGGC(G)-3′ (Husbands et al., 2007). The function of many *LBD* genes is still unknown and their expression patterns are variable (Shuai et al., 2002; Majer and Hochholdinger, 2011; Mangeon et al., 2011; Mangeon et al., 2012). However, many of the *LBD* genes have expression patterns that are tissue specific or only expressed during certain stages of development (Semiarti et al., 2001; Shuai et al., 2002; Lin et al., 2003; Nakazawa et al., 2003; Borghi, 2007; Iwakawa, 2007; Naito et al., 2007; Okushima et al., 2007; Soyano et al., 2008; Lee et al., 2009; Rubin et al., 2009; Oh et al., 2010; Berckmans et al., 2011; Majer and Hochholdinger, 2011; Bell et al., 2012; Fan et al., 2012). It was also found that *LBD* genes are conserved in many other plant species such as maize and rice (Shuai et al., 2002; Liu et al., 2005; Bortiri et al., 2006; Yang et al., 2006; Evans, 2007; Taramino et al., 2007; Li et al., 2008; Ma et al., 2009; Chen et al., 2012; Wang et al., 2013). The functions of *LBD* genes include adventitious root formation and leaf development in rice, embryo sac and leaf development in maize and pulvinus formation in several legume species (Liu et al., 2005; Ma et al., 2009; Evans, 2007; Chen et al., 2012; Zhou et al., 2012).

The founding member of the LBD family, *LATERAL ORGAN BOUNDARIES* (*LOB*), was identified based on its expression pattern (Shuai et al., 2002).

*LOB* encodes a transcription factor that differentially regulates a variety of genes (Bell et al., 2012). From electrophoretic mobility shift assays, it was shown that LOB and other LBD proteins bind specifically to the LBD motif (Husbands et al., 2007). Another experiment supporting LOB's function as a transcription factor examined *35S:GFP–LOB* plants to determine LOB's subcellular localization (Husbands et al., 2007). GFP fluorescence was detected in the nucleus, consistent with the hypothesis that LOB functions as a transcription factor (Husbands et al., 2007). To determine the expression pattern of *LOB*, plants were transformed with a *LOB* promoter:reporter fusion construct, *pLOB:GUS* (Shuai et al., 2002). Expression was found at the adaxial base of all lateral organs including the base of leaves, pedicels, lateral roots and floral organs (Shuai et al., 2002). *RAMOSA2* (*RA2),* the presumed LOB ortholog in maize, is expressed at the site of axillary meristem initiation and functions in controlling inflorescence branching by limiting growth of axillary meristems (Bortiri et al., 2006).

LOB plays a role in organ separation by limiting growth in the boundary region (Bell et al., 2012). *LOB* overexpression resulted in plants that were overall smaller than wild type, with short petioles and lack of stem elongation, suggesting that LOB plays a role in limiting growth (Shuai et al., 2002). Loss-of-function *lob* mutants exhibit normal vegetative development, but display a fusion of the axillary stem to the cauline leaf (Bell et al., 2012). The relatively limited phenotype may indicate that LOB function is redundant. When examining cells in the fused region of the *lob-3* mutant, the cells appeared larger (Bell et al., 2012). Together these

results suggest LOB is involved in organ separation because *lob* mutants have an expansion or overgrowth of the boundary due to defects in growth limitation (Bell et al., 2012). Within this fused region of the *lob-3* mutant, boundary marker expression was detected, which suggests the fusion is not due to defects in cell fate specification (Bell et al., 2012).

It has also been shown that LOB negatively regulates brassinosteroid (BR) accumulation in the boundary region in order to limit growth through a feedback loop (Bell et al., 2012). This loop consists of BR positively regulating *LOB* expression, which in turn activates expression of *BAS1*, a BR-inactivating enzyme (Bell et al., 2012). This negative feedback loop makes apparent the importance of regulating growth in the boundary region. *BAS1* was identified as a target of LOB through microarray experiments and confirmed based on electrophoretic mobility shift assays, overlapping expression patterns and chromatin immunoprecipitation results (Bell et al., 2012). In addition to regulating BR-modulated genes, LOB was also found to regulate genes associated with cell wall modifications and stimulus responses (Bell et al, 2012). As of now, the functional significance of these additional targets of LOB remains to be investigated.

Two potential downstream targets of LOB identified in the microarray experiment were genes encoding trehalose phosphate phosphatases (Bell et al., 2012). To rapidly induce LOB activity, a construct, *p35S:LOB-GR* , which contains a translational fusion between LOB and the hormone-binding domain of glucocorticoid receptor (GR) driven by the *35S* promoter was introduced into

*Arabidopsis* (Bell et al., 2012). In this system, the LOB-GR fusion protein is sequestered in the cytoplasm unless a steroid is present (Bell et al., 2012). Treatment with the synthetic steroid dexamethasone (DEX) allows the LOB-GR fusion protein to be transported to the nucleus, where it can regulate gene expression. Following the DEX induction for four hours, RNA samples were hybridized to Affymetrix ATH1 arrays (Bell et al., 2012). In total, 288 transcripts were identified that respond to LOB activation based on a $\geq 2$ fold change of transcript after DEX induction (Bell et al., 2012). The differentially expressed genes are candidate direct targets of LOB regulation. Intriguingly, one of the differently expressed genes was *TPPJ* (Bell et al., 2012). TPPJ transcript induction was also observed when DEX induction was done in the presence of the protein synthesis inhibitor cycloheximide, suggesting that *TPPJ* is a direct target of LOB (Yu, unpublished). Because *TPPI* is a close paralog of *TPPJ* (Paul et al., 2008), this gene was also of interest. Together, these experiments suggest the possibility that LOB regulates *TPPI* and *TPPJ*. The relationship between *LOB* and *TPPI* and *TPPJ* are explored in this thesis.

**Role of Trehalose in Plant Development**

Trehalose is a stable disaccharide that consists of two glucose units linked in an α,α-1,1 configuration, which can be synthesized in all organisms except vertebrates (Paul et al., 2008). Because trehalose is a nonreducing disaccharide, it is highly resistant to heat and pH (Goddijn and van Dun, 1999; Wingler, 2002). The

trace abundance of trehalose 6-phosphate (T6P) and trehalose in plants has made this pathway difficult to study (Paul et al., 2008). One reason for the low abundance of trehalose compared to sucrose in plants may be due to transport efficiency based on solubility (Paul et al., 2008). Low abundance of trehalose and the presence of multiple copies of trehalose biosynthetic genes suggest they play a regulatory role (Leyman et al., 2001).

Trehalose and its metabolic intermediates are shown to have many functions such as carbohydrate storage, stress protection and metabolic regulation (Wingler, 2002; Paul et al., 2008; Smeekens et al., 2010; Eveland and Jackson, 2012; O'Hara et al., 2013). Since trehalose is very stable, it is an ideal stress protectant and is capable of stabilizing proteins and membranes when under stress (Leyman et al., 2001; Wingler, 2002). One intermediate of the trehalose pathway, T6P, plays a role in metabolic regulation by directing carbon fluxes to control pool sizes of uridine diphosphoglucose (UDPG), which is essential for cell wall synthesis (Paul et al., 2008; Ponnu et al., 2011; O'Hara et al., 2013). The regulatory role of T6P provides a link between plant metabolism and development because UDPG is critical for cellular functions (Paul et al., 2008; Ponnu et al., 2011; Eveland and Jackson, 2012; O'Hara et al., 2013). The specific role of trehalose is still not clear, but it may regulate starch breakdown (Paul et al., 2008). Plants may also use trehalose as a source to rapidly obtain glucose units (Leyman et al., 2001). Overall, many of the precursors of trehalose are involved in regulating metabolic processes in plants

(Wingler et al., 2002; Paul et al., 2008; Smeekens et al., 2010; Eveland and Jackson, 2012; O'Hara et al., 2013).

In plants, the only trehalose biosynthesis pathway that is known to exist is the OtsA-OtsB pathway (Paul et al., 2008). The pathway begins with the production of T6P by transferring glucose from UDPG to glucose 6-phosphate (G6P). This step is catalyzed by trehalose phosphate synthase (TPS). Next, trehalose phosphate phosphatase (TPP) dephosphorylates T6P to produce trehalose. Trehalose can then be broken down by trehalase into two glucose units (Paul et al., 2008; Smeekens et al., 2010).

Determination of the genome sequence of *Arabidopsis* revealed the existence of an abundance of genes for trehalose synthesis (Leyman et al., 2001). In total, 21 genes are involved in the synthesis of trehalose in *Arabidopsis* (Paul et al., 2008). Present in plants are two classes of *TPS* genes, two classes of *TPP* genes and one class of *trehalase* genes (Paul et al., 2008). Specifically in *Arabidopsis*, there are 11 *TPS* genes that are grouped based on their similarity to yeast genes (Leyman et al., 2001; Paul et al., 2008). TPPs make up a family of 10 genes and all have conserved amino acid motifs characteristic of the 2-haloacid dehalogenase superfamily of enzymes (Paul et al., 2008). In *Arabidopsis*, *TPPI* and *TPPJ* are most similar to each other and are thought to have arisen from a recent gene duplication event (Paul et al., 2008).

Support for *TPP* genes regulating plant architecture is based on studies of the *TPP* gene, *RAMOSA3* (*RA3*), in maize. *ra3* mutants produce axillary meristems in the

inflorescence that are indeterminate and enlarged (Satoh-Nagasawa et al., 2006). As a consequence, *ra3* mutants have defects in inflorescence branching and form ears with abnormally long branches. *RA3* is expressed in domains subtending axillary inflorescence meristems (Satoh-Nagasawa et al., 2006). Based on this, the authors proposed that *RA3* plays a role in controlling maize inflorescence branching through modification of a sugar signal that travels into axillary meristems. This is critical evidence supporting the link between plant development and the trehalose pathway. It is also likely that *RA3* function is conserved in other grasses, such as sorghum, based on expression patterns of *RA3* orthologs (Satoh-Nagasawa et al., 2006). This allows the possibility for future applications of these studies to other staple crops.

Additional studies have implicated members of the trehalose pathway in the transition from vegetative to reproductive development, which is a key developmental stage that determines the reproductive success of a plant. The role of *TREHALOSE-6-PHOSPHATE SYNTHASE 1 (TPS1*) in *Arabidopsis* was investigated by generating plants with reduced *TPS1* expression using an artificial microRNA (Wahl et al., 2013). This resulted in reduced T6P levels by 30% and caused an extreme delay in flowering (Wahl et al., 2013). Overall, the authors concluded that *TPS1* is required for the timely initiation of flowering by regulating the expression of key floral integrators. Previously, a role in embryo development had also been demonstrated for *TPS1,* where it functions to coordinate cell division and cell wall biosynthesis with metabolism (Gómez et al., 2006). *tps1* embryos arrest at the

torpedo stage due to decreased cell division rates and cell wall thickening (Gómez et al., 2006). These results emphasize how trehalose signaling can impact plant development.

**Support for the Role of TPPI and TPPJ in the Boundary Region**

As previously mentioned, *RA2* is the maize ortholog of *LOB* and *RA3* encodes a TPP (Bortiri et al., 2006; Satoh-Nagasawa et al., 2006). Both *ra3* and *ra2* mutants have defects in inflorescence architecture including additional branching and loss of determinacy in the ears and tassels (Bortiri et al., 2006; Satoh-Nagasawa et al., 2006). In addition to *ra2* and *ra3*, another mutant that results in similar branching defects is *ra1*. *RA1* encodes a putative zinc-finger transcription factor (Vollbrecht et al., 2005). Evidence from double mutant analysis and expression data, suggest that both *RA2* and *RA3* act upstream of *RA1* to regulate meristem identity and determinacy (Bortiri et al., 2006; Satoh-Nagasawa et al., 2006; Vollbrecht et al., 2005). Understanding the genetic control of inflorescence architecture is critical, because architecture traits are critical to yield in many of the staple crops. The thought that this relationship between *RA2* and *RA3* is conserved in *Arabidopsis* is particularly intriguing because of evidence that the RA2 ortholog LOB regulates *TPPJ*, which is related to *RA3* (Bell et al., 2012).

Based on publicly available microarray studies, the expression profile for many genes in the *Arabidopsis* genome can be queried in several databases (Schmid et al., 2005; Winter et al., 2007; Yadav et al., 2009). The electronic Fluorescent Pictograph

(eFP) Browser that compiles large-scale data sets, such as microarray data, allows for a user-friendly visualization of collected data in a pictograph form (Winter et al., 2007). Examination of *TPPI* and *TPPJ* in the eFP browser revealed that *TPPI* transcript levels are highest in the carpels, siliques and seeds and *TPPJ* transcript levels are highest in developing seeds during the cotyledons stage (Winter et al., 2007). To identify transcript expression patterns in discrete regions of the SAM, an expression profiling method was used that allows detection of expression patterns specific to cells in individual spatial domains of SAMs (Yadav et al., 2009). The results showed that *TPPI* transcript levels are highest in the peripheral zone and *TPPJ* transcript levels are high throughout the SAM (Yadav et al., 2009). This pattern is overlapping when compared to *pLOB:GUS* expression, which provides support for LOB's potential to regulate *TPPI* and *TPPJ* (Shuai et al., 2002).

The overall objective of this research was to investigate the function of *TPPI* and *TPPJ* in the boundary region of *Arabidopsis*. To address this, the following two main goals were considered. The first goal was to characterize *TPPI* and *TPPJ* T-DNA mutants. To accomplish this, mutants were observed for phenotypic changes and transcript levels were determined. The second goal was to examine the relationship between *LOB* and *TPPI* and *TPPJ* by using genetic and transgenic approaches. To further investigate the relationship between *LOB* and *TPPI*, a *lob-3 tppi-1* double mutant was generated and analyzed for any changes in fusion phenotypes. To determine if decreased levels of *TPPJ* causes fusion and if *TPPJ* can rescue the *lob-3* fusion phenotype, *pLOB:TPPJ-3'UTR* transgenic plants were generated. These

transgenic plants were examined for changes in fusion within the boundary region. The objective was for these experiments to further determine if LOB plays a role in regulating *TPPI* or *TPPJ* within the boundary region. A broader objective for this study was to provide evidence of whether or not the relationship between LOB and TPPs in maize is also conserved in *Arabidopsis.*

## Results

### *tppj-sk* Is A Hypomorphic Mutation

To investigate *TPPJ* function, we characterized *tppj-sk,* a T-DNA allele from the Saskatoon Arabidopsis collection (Robison and Parkin, 2009). This line has an activation-tagging T-DNA insertion containing outward-reading *35S* enhancer elements (Robison and Parkin, 2009). In *tppj-sk,* the T-DNA insertion is 300bp upstream of the *TPPJ* ATG site (Figure 1) and was therefore expected to result in increased *TPPJ* transcript levels.

To determine if the T-DNA insertion caused an increase in *TPPJ* activity, *TPPJ* transcript levels were examined in *tppj-sk* mutants and wild-type *Col-0* plants. RNA was isolated from pools of primary inflorescences and paraclade junctions on the primary stem. Inflorescences were collected because *TPPJ* transcript levels are highest in the peripheral zone of the SAM (Yadav et al., 2009). The third paraclade junctions on the primary stem were collected because fusion is present at this boundary in *lob-3* mutants, signifying high *LOB* activity (Bell et al., 2012). If *TPPJ* is a direct target of *LOB*, then *TPPJ* and *LOB* expression should partially overlap. Tissue

samples were collected from *Col-0* and *tppj-sk* plants and transcript levels were examined using RT-PCR and gene-specific primers (Figure 2). Examination of *TPPJ* transcript levels in inflorescences revealed that the *tppj-sk* mutant had lower levels of *TPPJ* transcript compared to wild type. In paraclade junctions, *TPPJ* transcript levels were also lower in *tppj-sk* mutants compared to wild type. These data show that the *tppj-sk* mutant does not have elevated *TPPJ* transcript levels as expected for an activation-tagged line. Thus, in this instance, the T-DNA insertion is not acting as an activation tag to *TPPJ*, but rather resulted in reduced transcript levels, perhaps due to the disruption of an upstream regulatory element. Although *TPPJ* transcripts were decreased in *tppj-sk*, it is important to note that they were still detected, therefore this insertion results in a hypomorphic *TPPJ* allele.

**Expression of *TPPJ* in *lob-3***

Previous microarray experiments suggested *TPPJ* to be a target of LOB transcriptional regulation (Bell et al., 2012). *TPPJ* transcript levels were increased approximately 2.5 fold after induction of LOB activity (Bell et al., 2012). If LOB positively regulates *TPPJ* expression, then transcript levels might be reduced in *lob* loss-of-function mutants. To determine whether *TPPJ* transcript levels were altered in the *lob-3* mutant, RT-PCR was performed. RNA was isolated from inflorescences and paraclade junctions of *Col-0* and *lob-3* plants and *TPPJ* transcript levels were examined using RT-PCR and gene-specific primers (Figure 2). In *Col-0* and *lob-3* inflorescence and paraclade junction samples, *TPPJ* transcript levels were similar

(Figure 2). However, in one of the three biological replicates, *TPPJ* transcript levels were slightly higher in *lob-3* mutant inflorescences (Figure 2). These results are inconsistent with the previous microarray and qRT-PCR results, which showed an increase in *TPPJ* transcript levels in response to *LOB* misexpression in *p35S:LOB-GR* seedlings (Bell et al., 2012; Yu, unpublished). From the results, it can be concluded that *TPPJ* transcript levels were not altered in the *lob-3* mutant as would have been expected if LOB positively regulates *TPPJ*. A possible explanation for the results is that LOB may act redundantly to regulate *TPPJ* expression.

**Reduction in *TPPJ* Transcript Levels in *tppj-sk* Does Not Result in Phenotypic Changes**

To investigate the developmental role of *TPPJ* in *Arabidopsis*, we examined the hypomorphic *tppj-sk* mutant for phenotypic changes compared to wild-type plants. Because *TPPJ* transcript levels increased as a response to LOB activation (Bell et al., 2012), a reduction in TPPJ activity might be expected to result in phenotypes similar to those of *lob* mutants. To identify *tppj-sk* homozygous mutants, PCR-based genotyping was performed with the insert-specific primers pSKTAIL-L3 and a *TPPI* gene-specific primer At5g65140R RT (Table 1). *tppj-sk* mutants were examined during all stages of development specifically for fusion phenotypes in both leaves and floral organs, rosette leaf shape and overall architecture. No phenotypic differences were observed when comparing *tppj-sk* mutants to wild-type plants. Because *TPPJ* transcript levels were reduced, but not abolished, in the *tppj-sk*

mutant, the remaining *TPPJ* transcript may be sufficient for function; this could explain the lack of a phenotype in the *tppj-sk* mutant.

**Expression of *TPPJ* in the Boundary Can Suppress the *lob-3* Fusion**

If LOB positively regulates *TPPJ*, it is hypothesized that reduced *TPPJ* activity in *lob* loss-of-function mutants contributes to the observed fusion phenotype (Bell et al., 2012). To test the consequences of increased *TPPJ* levels specifically in the boundary, *TPPJ* was driven by the *LOB* promoter (*pLOB:TPPJ*) in *Col-0* and *lob-3* mutant plants. It is predicted that when *TPPJ* is driven by the *LOB* promoter, *TPPJ* will be able to replace LOB function. However, RT-PCR results show *TPPJ* levels were not decreased in the *lob-3* mutant, which is inconsistent with the hypothesis and may be due to sensitivity issues.

Altogether, 18 *Col-0* and 11 *pLOB:TPPJ* transgenic plants were identified in the $T_1$ generation. With the generous help of Robert Koble, a lab member, fusion phenotypes were observed by eye and measurements were recorded using a digimatic caliper. No significant difference was observed when comparing the contact between the cauline leaf and axillary stem in 8 *Col-0* and 8 *pLOB:TPPJ* in *Col-0* plants (Figures 3 and 4). The transgenic plants had clear boundary separation, which suggests the presumed higher levels of *TPPJ* in the boundary did not cause any phenotypic changes. Additionally, transgenic *lob-3 pLOB:TPPJ* plants showed a suppression of the fusion between the cauline leaf and axillary stem seen in *lob-3* plants (Figures 3 and 4). Fusion measurements taken from *lob-3* plants were

significantly different than the other genotypes (Figure 4). *lob-3* plants had an average fusion between the cauline leaf and axillary stem of 0.86 mm, whereas *pLOB:TPPJ* plants average contact length measured 0.29 mm (Figure 4). These results indicate that expression of *TPPJ* in the boundary can suppress the fusion in *lob-3* mutants, which is consistent with the hypothesis that LOB positively regulates *TPPJ*. This shows that *TPPJ* is sufficient to rescue the *lob* mutant phenotype, indicating trehalose signaling plays a role in organ separation. Further, these results suggest that lower levels of *TPPJ* RNAs in the *lob-3* mutants results in organ fusion. However this is in disagreement with the RT-PCR experiments, which did not detect reduced *TPPJ* levels in the *lob-3* mutants. A possible explanation for this contradiction may be that under the conditions used, the RT-PCR experiments were unable to detect significant changes because of low *TPPJ* transcript levels. The potential decrease in *TPPJ* levels in *lob-3* mutants may not be significant enough to be detected on a gel and therefore, the results show no change as expected. It is also important to note that different backgrounds and tissues were used for the microarray versus the RT-PCR.

**TPPI Plays A Role In Organ Separation**

TPPI is a closely related paralog of TPPJ (Paul et al., 2008). To investigate the developmental role of TPPI in *Arabidopsis*, *tppi-1* mutants were obtained from the Syngenta Arabidopsis Insertion Library collection (Sessions et al., 2002). *tppi-1* mutants contain a T-DNA inserted within the fourth exon of *TPPI* (Figure 5). To

identify *tppi-1* homozygous mutants, PCR-based genotyping was performed with gene-specific primers At5g10100F and LB3 (Table 1). When observing the plants for phenotypic changes, we saw fusion of the cauline leaf to the main stem, which is known as a decurrent strand (Emery et al., 2003), in the *tppi-1* mutants (Figure 6). The decurrent strand tissue is continuous with the cauline leaf and the stipule, marking the base of the leaf, can be located at the base of these strands. The decurrent strand represents an expansion of the boundary between the leaf and main stem. This fusion differs from that seen in *lob-3* mutants, where the cauline leaf is fused to the axillary stem (Bell et al., 2012). The presence of decurrent strands in *tppi-1* mutants suggests that TPPI plays a role in organ separation.

To examine the consequences of the T-DNA insertion on *TPPI* transcript levels, RT-PCR was performed. RNA was isolated from pools of primary inflorescences and the third paraclade junction on the primary stem. Tissue samples were collected from *Col-0*, *lob-3*, *tppi-1*, and *lob-3 tppi-1* plants. After cDNA was synthesized, RT-PCR was attempted. Unfortunately, RT-PCR results were not obtained due to difficulties in detecting *TPPI* transcripts in any of the genotypes. One explanation for this may be due to naturally low levels of *TPPI* transcript, making it difficult to detect. Due to the sequence similarity between *TPPI* and *TPPJ*, it was also difficult to design specific primers.

**The T-DNA Insertion Co-segregates With the Decurrent Strand Phenotype in *tppi-1***

To determine if the presence of decurrent-strands in *tppi-1* mutants was a result of the T-DNA insertion, a backcross was performed between *TPPI/TPPI* and *tppi-1* plants. To determine if the decurrent strand phenotype segregated with the T-DNA insertion, fusion phenotypes were recorded on segregating F2 populations (Figure 6). In total, the measured $F_2$ generation consisted of 16 *TPPI/TPPI* plants, 27 *TPPI*/*tppi-1* heterozygous plants and 10 *tppi-1* homozygous plants. Measurements were taken using a digimatic caliper at the stage in which plants had 25 flowers on their primary inflorescence. When comparing the contact between the cauline leaf and axillary stem, significant differences were not abundant. Only in cauline leaf 2 and 3 was the fusion significantly longer in *tppi-1* homozygous plants compared to *TPPI/TPPI* (Figure 7). There is a significant difference when comparing the frequency of plants with decurrent-strands (Figure 8). The decurrent strand phenotype was oberserved most frequently in the *tppi-1* homozygous mutants, however one *TPPI/TPPI* plant also had a decurrent strand present (Figure 8). All *tppi-1* homozygous plants had decurrent strands present on either the main stem or the axillary stem or both. Statistical tests could not be done when comparing the lengths of the decurrent strands due to the limited number of *TPPI/TPPI* plants with decurrent strands (Figure 9). The presence of a decurrent strand in one *TPPI/TPPI* plant may indicate that the T-DNA insertion in the *tppi-1* line is not the cause of the fusion phenotype. The presence of a decurrent strand in

a *TPPI/TPPI* plant may be due to a closely linked mutation. To investigate this further, a functional copy of *TPPI* should be introduced into the *tppi-1* mutant to determine if the decurrent-strand phenotype can be complemented.

### *tppi-1* and *lob-3 tppi-1* Plants Have Delayed Flowering

The decurrent-strand phenotype we observed in *tppi-1* mutants indicates that *TPPI* has a role in organ separation. To investigate a possible genetic relationship between *TPPI* and *LOB*, *lob-3 tppi-1* double mutants were generated. If *LOB* and *TPPI* are in the same genetic pathway, then an enhancement of the fusion between the axillary stem and cauline leaf might be expected in the double mutant. Fusion phenotypes were recorded in both single mutants and double homozygous mutants generated from the $F_3$ and $F_4$ generation (Figure 10). These generations were analyzed to ensure expected segregation ratios, confirm no embryo lethality and to observe consistent phenotypes over multiple generations. The measured $F_4$ generation consisted of *LOB/LOB TPPI/TPPI*, *lob-3*, *tppi-1* and *lob-3 tppi-1* plants. Measurements were taken using a digimatic caliper once the plants had 25 flowers on their primary inflorescence. When examining the contact between the cauline leaf and axillary stem, *lob-3 tppi-1* double mutants were generally not significantly different than *lob-3*. Only in cauline leaf 1 was the fusion significantly longer in *lob-3 tppi-1* plants compared to *lob*-3 plants (Figure 11). This could possibly be due to higher levels of *TPPI* in this region or that the *lob-3* phenotype is more severe in the higher cauline leaf axils. When comparing the lengths of the decurrent strands on

the *tppi-1* and *lob-3 tppi-1* plants, there was no significant difference (Figure 12). However, the decurrent-strand phenotype was only present on *tppi-1* and *lob-3 tppi-1* plants and not *LOB/LOB TPPI/TPPI*. Since no enhancements in fusion were observed in *lob-3 tppi-1* plants, it suggests that neither *LOB* nor *TPPI* require the other for their roles in organ separation. It is also important to note that all the *tppi-1* (one exception) and *lob-3 tppi-1* plants had much rounder and darker rosette leaves compared to wild type plants (Figure 10). Additionally, the *tppi-1* and *lob-3 tppi-1* plants flowered significantly later (one week) compared to *LOB/LOB TPPI/TPPI* plants (Figure 13). This result indicates that *TPPI* plays a role in the transition from vegetative to reproductive development, because *lob-3* mutants do not exhibit late flowering. The transition from vegetative to reproductive development is a significant stage because it can determine a plant's success.

**Discussion**

When analyzing *tppj-sk* mutants, it was discovered that they have decreased levels of *TPPJ* transcript. Because this line contains an activation tagging T-DNA positioned upstream of the coding region, this line was expected to have increased levels of *TPPJ* transcript. Instead, the T-DNA insertion caused reduced *TPPJ* transcript levels, perhaps due to the disruption of an upstream regulatory element. It also appears that overall, *TPPJ* transcript levels are low in the tissues sampled. Although *TPPJ* transcript levels increased in response to *LOB* overexpression, which suggested that LOB positively regulates TPPJ (Bell et al., 2012). The expression

analyses presented here indicated that *TPPJ* transcript levels were unaltered in the *lob-3* mutant. This discrepancy could be due to the fact that misexpression under the *35S* promoter resulted in artefactual regulation, perhaps due to the presence of additional co-factors that are not normally present in the boundary regions. It may also be due to issues with the specificity of the primers used for RT-PCR. Additionally, it was discovered that *pLOB:TPPJ* rescues the *lob-3* fusion phenotype. This finding suggests that lower levels of *TPPJ* in the *lob-3* mutants results in organ fusion, consistent with the hypothesis that LOB positively regulates *TPPJ.* Excluding the RT-PCR results (Figure 2), all other findings suggests LOB positively regulates *TPPJ* and *TPPJ* levels are decreased in *lob* mutants. Since lower *TPPJ* levels were not detected in the *lob-3* mutants as expected, but *TPPJ* was sufficient to rescue the *lob* mutant phenotype, the RT-PCR results may be inconclusive due to sensitivity issues. This could be due to the changes in *TPPJ* levels in *lob-3* mutants not being significant enough to be detected on a gel. To confirm these results, it would be beneficial to perform qRT-PCR to obtain more accurate data. It is also important to note that *p35S:LOB-GR* seedlings were used for the microarray, whereas *lob-3* inflorescence and paraclade junctions were used for the RT-PCR. Overall, TPPJ may be involved in many functions including organ separation and therefore may be regulated by many different pathways.

To continue this work, it would be beneficial to observe additional plants with altered levels of *TPPJ*. First, the homozygotes in the $T_2$ generation of the *pLOB:TPPJ* transgenic plants need to be examined. This will be essential to verify

the rescue phenotypes seen in the $T_1$ generation. Additional support for this study would be to observe *lob-3 tppj-sk* double mutants. These crosses have been made, but homozygotes still need to be identified in the $F_2$ generation. If fusion phenotypes in the double mutants differ from the *lob-3* mutants, then it would provide support that *TPPJ* and *LOB* have overlapping pathways. Additional tissues should also be sampled using RT-PCR for the possibility of clearer results. Other tissues may have higher levels of *TPPJ* transcript, which would allow for better detection. It would also be beneficial to observe a *TPPJ* null mutant to identify any phenotypic changes. This might provide further information regarding the role of TPPJ.

TPPI appears to play a similar role to LOB in organ separation. The presence of decurrent strands in *tppi-1* plants suggests this role in organ separation. However it is important to note the occurrence of a decurrent strand in a wild-type plant generated from the backcross with *tppi-1*. This may mean that the T-DNA insertion in the *tppi-1* line is not the cause of the fusion phenotype. Instead, the presence of decurrent strands may be due to a closely linked mutation. To investigate this further, a functional copy of *TPPI* should be inserted into the *tppi-1* mutant to see if the decurrent strand phenotype is rescued. Since no changes in fusion were observed in *lob-3 tppi-1* plants compared to *lob-3* and *tppi-1* mutants, it suggest that neither *LOB* nor *TPPI* require the other for their roles in organ separation. TPPI also may be involved in flowering time due to the delays in flowering of the *tppi-1* plants compared to wild type. This result is not surprising

because other trehalose mutants have also been shown to flower extremely late (Wahl et al., 2013).

To further determine the function of TPPI, it would be beneficial to investigate with transgenic plants using a *pLOB:TPPI-3'UTR* construct. Observing these transgenic plants would help determine the consequences of increased *TPPI* levels specifically in the boundary. Because the RT-PCR was unsuccessful, it is unknown if the *tppi-1* mutant is a null. By obtaining these results, further investigation of the developmental role of TPPI in *Arabidopsis* can be performed. Additionally, it would be interesting to look at a cellular level at the decurrent strands in *tppi-1* plants. This would provide further detail about the characteristics of the fusion and possible roles of TPPI.

Together, this work provides a starting point for determining the function of TPPI and TPPJ in the boundary region of *Arabidopsis*. Because other boundary gene mutants also have decurrent-strand phenotypes, it may be possible that TPPI interacts with one of these genes. Boundary genes to consider are *LOF1* and *LOF2* because the *lof1 lof2* double mutant displays decurrent strands (Lee et al., 2009). It is possible that these genes are part of similar pathways that function in separating the cauline leaf from the main stem. *REVOLUTA*, a gene that limits cell division in leaves and stems, is also of interest (Emery et al., 2003). *rev-10d* plants, which contain a semidominant gain-of-function *REV* allele, also display decurrent strands (Emery et al., 2003). The first step to investigate these genes would be to determine if they have overlapping expression patterns when compared to *TPPI.* As previously

discussed, both *RA2*, an ortholog of *LOB*, and *RA3*, which encodes a TPP in maize, act upstream of *RA1* and play a role in regulating maize inflorescence branching (Bortiri et al., 2006; Satoh-Nagasawa et al., 2006; Vollbrecht et al., 2005). It appears from this study that this relationship is also conserved in *Arabidopsis,* because both LOB and TPPJ play a role in regulating organ separation. The knowledge gained from studying these pathways in *Arabidopsis*, will be insightful to understanding regulation of shoot architecture in maize and possibly other staple crop plants. Overall, the goal is to apply this knowledge of shoot architecture regulation to manipulate traits such as inflorescence branching to increase yields.

## Materials and Methods

### Plant Materials

T-DNA insertional mutants *lob-3* (SALK_042599), *tppi-1* (SAIL_354_D09) and *tppj-sk* (sk476) were obtained from the SALK T-DNA collection, Syngenta Arabidopsis Insertion Library collection and Saskatoon Arabidopsis collection respectively (Robison and Parkin, 2009; Alonso et al., 2003; Sessions et al., 2002; Robison and Parkin, 2009). *lob-3* mutants contain a T-DNA inserted at the 3'UTR of *LOB* (Bell et al., 2012). *tppi-1* mutants contain a T-DNA inserted within *TPPI* (Figure 5). *tppj-sk* mutants contain a T-DNA inserted upstream of the ATG site of *TPPJ* (Figure 1). *lob-3* homozygous mutants were identified by PCR-based genotyping with gene-specific primers Lba1 and LOB-RKR (Table 1). *tppi-1* homozygous mutants were identified by PCR-based genotyping with gene-specific primers

At5g10100F and LB3 (Table 1). *tppj-sk* homozygous mutants were identified by PCR-based genotyping with gene specific primers pSKTAIL-L3 and At5g65140R (Table 1). The *lob-3 tppi-1* double mutants were generated by crossing *lob-3* with *tppi-1* and homozygous mutants were identified in the F2 generation using the previously mentioned primers for genotyping.

**Growth Conditions**

All *Arabidopsis* plants used in this experiment were soil-grown in Sunshine LC1 Mix. Before planting, all seeds were surface-sterilized with 95% ethanol. Lights in the growth rooms were set to 16-hours light, 8-hours dark and temperatures were set at 22°C.

**Phenotypic Analyses**

Measurements of contact length between the stems and cauline leaves were taken using a digimatic caliper. Measurements were taken on the primary stem when 25 flowers had formed on the primary inflorescence. L1 corresponds to the lowest cauline leaf axil on the main stem and L2 corresponds to the next one above L1. All statistical analyses were done using a Student's T-Test on MS Excel. Images were taken using a Leica MZ8 stereo microscope.

**RT-PCR Analysis**

RNA was isolated from pools of primary inflorescences and paraclade junctions (PJ3 on primary stem) tissue of *Arabidopsis* plants using TRIzol reagent (Invitrogen). cDNA was synthesized from 2-3 µg of total RNA using an oligo (dT) primer and Superscript Reverse Transcriptase (Invitrogen). RNA concentrations and quality were measured using a NanoDrop. For reverse transcriptase–mediated PCR, *TPPJ* was amplified using At5g65140F RT and At5g65140R RT primers (Table 1). For an equal loading control, *ACTIN2* was amplified with ACT2-C and ACT2-N primers (Table 1). PCR conditions for *TPPJ* amplification were as follows: denaturation at 94°C for 3 min, followed by 30 cycles of 94°C for 30 s, 57°C for 30 s, and 72°C for 1 min. PCR conditions for *ACT2* amplification were as follows: denaturation at 94°C for 3 min, followed by 25 cycles of 94°C for 30 s, 55°C for 30 s, and 72°C for 90 s.

**Plasmid Constructs**

Using the Gateway cloning system, *pLOB:Frame A-3'UTR* was constructed by a previous lab member (Yu, unpublished). Coding sequences of *TPPI* (At5g10100) and *TPPJ* (At5g65140) were amplified from *Col* cDNA using TPPI F and TPPI R-GW and TPPJ F and TPPJ R primers respectively (Table 1). The fragments were ligated into pENTR-TOPO (Invitrogen) to generate *TPPI-pENTR* and *TPPJ-pENTR*. Both constructs were sequenced at UCR Genomics Core to confirm their integrity. *pLOB:TPPJ-3'UTR* was generated by performing a recombination reaction between

*pLOB:Frame A-3'UTR* and *TPPJ-pENTR* using LR Clonase (Invitrogen). The construct was introduced into *Agrobacterium tumefaciens* strain GV3101 and *Col-0*, *lob-3*, *Ler*, *Et22 Arabidopsis* plants were transformed by floral dip (Clough et al., 1998). For selection purposes, plants were sprayed with a 1:2000 dilution of BASTA (0.1 g/L Glufosinate-ammonium) and survivors were genotyped to confirm.

## References


Aida, M., Ishida, T., & Tasaka, M. (1999). Shoot apical meristem and cotyledon formation during *Arabidopsis* embryogenesis: interaction among the *CUP-SHAPED COTYLEDON* and *SHOOT MERISTEMLESS* genes. *Development, 126*(8), 1563-1570.

Aida, M., Ishida, T., Fukaki, H., Fujisawa, H., & Tasaka, M. (1997). Genes involved in organ separation in *Arabidopsis*: an analysis of the cup-shaped cotyledon mutant. *Plant Cell, 9*(6), 841-857.

Alonso, J. M., et al. (2003). Genome-wide insertional mutagenesis of *Arabidopsis thaliana*. *Science, 301*(5633), 653-657.

Barton, M. K. (2010). Twenty years on: The inner workings of the shoot apical meristem, a developmental dynamo. *Dev Biol, 341*(1), 95-113.

Bell, E. M., et al. (2012). *Arabidopsis* LATERAL ORGAN BOUNDARIES negatively regulates brassinosteroid accumulation to limit growth in organ boundaries. *Proc Natl Acad Sci USA, 109*(51), 21146-21151.

Berckmans, B., et al. (2011). Auxin-dependent cell cycle reactivation through transcriptional regulation of *Arabidopsis E2Fa* by lateral organ boundary proteins. *Plant Cell*, 23(10), 3671-3683.

Borghi, L., Bureau, M., & Simon, R. (2007). *Arabidopsis JAGGED LATERAL ORGANS* is expressed in boundaries and coordinates *KNOX* and *PIN* activity. *Plant Cell, 19*(6), 1795-1808.

Bortiri, E., Chuck, G., Vollbrecht, E., Rocheford, T., Martienssen, R., & Hake, S. (2006). *ramosa2* encodes a LATERAL ORGAN BOUNDARY domain protein that determines the fate of stem cells in branch meristems of maize. *Plant Cell, 18*(3), 574-585.

Breuil-Broyer, S., Morel, P., De Almeida-Engler, J., Coustham, V., Negrutiu, I., & Trehin, C. (2004). High-resolution boundary analysis *during Arabidopsis thaliana* flower development. *Plant J, 38*(1), 182-192.

Chen, J., Moreau, C., Liu, Y., Kawaguchi, M., Hofer, J., Ellis, N., & Chen, R. (2012). Conserved genetic determinant of motor organ identity in *Medicago truncatula* and related legumes. *Proc Natl Acad Sci USA, 109*(29), 11723-11728.

Clough, S. J., & Bent, A. F. (1998). Floral dip: a simplified method for *Agrobacterium*-mediated transformation of *Arabidopsis thaliana*. *Plant J, 16*(6), 735-743.

Duvick, D. (2005). Genetic progress in yield of United States maize (*Zea mays* L.). *Maydica* 50, 193–202.

Emery, J., Floyd, S., Alvarez, J., Eshed, Y., Hawker, N., Izhaki, A., Baum, S., & Bowman, J. (2003). Radial patterning of *Arabidopsis* shoots by class III HD-ZIP and KANADI genes. *Curr Biol,* 13(20), 1768–1774.

Evans, M. M. S. (2007). The *indeterminate gametophyte1* gene of maize encodes a LOB domain protein required for embryo sac and leaf development. *Plant Cell, 19*(1), 46-62.

Eveland, A., & Jackson, P. (2012). Sugars, signalling, and plant development. *J Exp Bot*, 63(9), 3367-3377.

Fan, M., Xu, C., Xu, K., & Hu, Y. (2012). LATERAL ORGAN BOUNDARIES DOMAIN transcription factors direct callus formation in *Arabidopsis* regeneration. *Cell Res*, 22(7), 1169–80.

Goddijn, O. J. M., & van Dun, K. (1999). Trehalose metabolism in plants. *Trends Plant Sci, 4*(8), 315-319.

Gómez, L. D., Baud, S., Gilday, A., Li, Y., & Graham, I. A. (2006). Delayed embryo development in the *ARABIDOPSIS TREHALOSE-6-PHOSPHATE SYNTHASE 1* mutant is associated with altered cell wall structure, decreased cell division and starch accumulation. *Plant J, 46*(1), 69-84.

Greb, T., Clarenz, O., Schäfer, E., Müller, D., Herrero, R., Schmitz, G., & Theres, K. (2003). Molecular analysis of the *LATERAL SUPPRESSOR* gene in *Arabidopsis* reveals a conserved control mechanism for axillary meristem formation. *Genes Dev, 17*(9), 1175-1187.

Ha, C. M., Kim, et al. (2003). The *BLADE-ON-PETIOLE 1* gene controls leaf pattern formation through the modulation of meristematic activity in *Arabidopsis*. *Development, 130*(1), 161-172.

Hepworth, S. R., Zhang, Y., McKim, S., Li, X., & Haughn, G. W. (2005). BLADE-ON-PETIOLE–dependent signaling controls leaf and floral patterning in *Arabidopsis*. *Plant Cell, 17*(5), 1434-1448.

Husbands, A., Bell, E. M., Shuai, B., Smith, H. M. S., & Springer, P. S. (2007). LATERAL ORGAN BOUNDARIES defines a new family of DNA-binding transcription factors and can interact with specific bHLH proteins. *Nucleic Acids Res, 35*(19), 6663-6671.

Hussey, G. (1971). Cell division and expansion and resultant tissue tensions in the shoot apex during the formation of a leaf primordium in tomato. *J Exp Bot, 22*(3), 702-714.

Iwakawa, H., et al. (2007). Expression of the *ASYMMETRIC LEAVES2* gene in the adaxial domain of *Arabidopsis* leaves represses cell proliferation in this domain and is critical for the development of properly expanded leaves. *Plant J,* 51, 173–84.

Jinn, T.-L., Stone, J. M., & Walker, J. C. (2000). *HAESA*, an *Arabidopsis* leucine-rich repeat receptor kinase, controls floral organ abscission. *Genes Dev, 14*(1), 108-117.

Keller, T., Abbott, J., Moritz, T., & Doerner, P. (2006). *Arabidopsis REGULATOR OF AXILLARY MERISTEMS1* controls a leaf axil stem cell niche and modulates vegetative development. *Plant Cell*, 18(3), 598-611.

Lee, D.-K., Geisler, M., & Springer, P. S. (2009). *LATERAL ORGAN FUSION1* and *LATERAL ORGAN FUSION2* function in lateral organ separation and axillary meristem formation in *Arabidopsis*. *Development, 136*(14), 2423-2432.

Lee, H.W., Kim, N.Y., Lee, D.J., & Kim, J. (2009). *LBD18/ASL20* regulates lateral root formation in combination with *LBD16/ASL18* downstream of *ARF7* and *ARF19* in *Arabidopsis*. *Plant Physiol*, 151(3), 1377–1389.

Leyman, B., Van Dijck, P., & Thevelein, J. M. (2001). An unexpected plethora of trehalose biosynthesis genes in *Arabidopsis thaliana*. *Trends Plant Sci, 6*(11), 510-513.

Li, A., et al. (2008). DH1, a LOB domain-like protein required for glume formation in rice. *Plant Mol Biol, 66*(5), 491-502.

Lin, W., Shuai, B., & Springer, P.S. (2003). The Arabidopsis *LATERAL ORGAN BOUNDARIES*-domain gene *ASYMMETRIC LEAVES2* functions in the repression of *KNOX* gene expression and in adaxial-abaxial patterning. *Plant Cell,* 15(10), 2241–2252.

Liu, H., et al. (2005). ARL1, a LOB-domain protein required for adventitious root formation in rice. *Plant J, 43*(1), 47-56.

Ma, Y., Wang, F., Guo, J., & Zhang, X. (2009). Rice *OsAS2* gene, a member of LOB domain family, functions in the regulation of shoot differentiation and leaf development. *J Plant Biol, 52*(5), 374-381.

Majer, C., & Hochholdinger, F. (2011). Defining the boundaries: structure and function of LOB domain proteins. *Trends Plant Sci*, 16(1), 47–52.

Mangeon, A., Lin, W.C., & Springer, S. (2012). Functional divergence in the *Arabidopsis* LOB-domain gene family. *Plant Signal Behav,* 7(12):1544-7.

Mangeon, A., Bell, E.M., Lin, W.C., Jablonska, B., & Springer, PS. (2011). Misregulation of the LOB domain gene *DDA1* suggests possible functions in auxin signalling and photomorphogenesis. *J Exp Bot*, 62(1), 221–33.

Müller, D., Schmitz, G., & Theres, K. (2006). *Blind* homologous *R2R3 Myb* genes control the pattern of lateral meristem initiation in *Arabidopsis*. *Plant Cell, 18*(3), 586-597.

Naito, T., Yamashino, T., Kiba, T., Koizumi, N., Kojima, M., Sakakibara, H., & Mizuno, T. (2007). A link between cytokinin and ASL9 (ASYMMETRIC LEAVES 2 LIKE 9) that belongs to the AS2/LOB (LATERAL ORGAN BOUNDARIES) family genes in *Arabidopsis thaliana*. *Biosci Biotechnol Biochem*, 71(5), 1269–1278.

Nakazawa, M., Ichikawa, T., Ishikawa, A., Kobayashi, H., Tsuhara, Y., Kawashima, M., Suzuki, K., Muto, S., & Matsui, M. (2003). Activation tagging, a novel tool to dissect the functions of a gene family. *Plant J*, 34(5), 741–750.

O'Hara, L., Paul, M., & Wingler, A. (2013). How do sugars regulate plant growth and development? New insight into the role of trehalose-6-phosphate. *Mol Plant*, 6(2), 261-274.

Oh, S.A., Park, K.S., Twell, D., & Park, S.K. (2010). The *SIDECAR POLLEN* gene encodes a microspore-specific LOB/AS2 domain protein required for the correct timing and orientation of asymmetric cell division. *Plant J*, 64(5), 839–50.

Okushima, Y., Fukaki, H., Onoda, M., Theologis, A., & Tasaka, M. (2007). ARF7 and ARF19 regulate lateral root formation via direct activation of *LBD/ASL* genes in *Arabidopsis*. *Plant Cell,* 19(1), 118–130.

Paul, M. J., Primavesi, L. F., Jhurreea, D., & Zhang, Y. (2008). Trehalose metabolism and signaling. *Annu Rev of Plant Biol, 59*(1), 417-441.

Ponnu, J., Wahl, V., & Schmid, M. (2011). Trehalose-6-phosphate: connecting plant metabolism and development. *Front Plant Sci*, 70(2).

Raman, S., Greb, T., Peaucelle, A., Blein, T., Laufs, P., & Theres, K. (2008). Interplay of miR164, *CUP-SHAPED COTYLEDON* genes and *LATERAL SUPPRESSOR* controls axillary meristem formation in *Arabidopsis thaliana*. *Plant J*, 55(1), 65-76.

Rast, M. I., & Simon, R. (2012). *Arabidopsis JAGGED LATERAL ORGANS* acts with *ASYMMETRIC LEAVES2* to coordinate *KNOX* and *PIN* expression in shoot and root meristems. *Plant Cell, 24*(7), 2917-2933.

Rast, M. I., & Simon, R. (2008). The meristem-to-organ boundary: more than an extremity of anything. *Curr Opin in Genet Dev, 18*(4), 287-294.

Robinson, S.J., & Parkin, I.A.P. (2009). Bridging the gene-to-function knowledge gap through functional genomics. *Methods Mol Biol*, 513, 153-73.

Rubin, G., Tohge, T., Matsuda, F., Saito, K., & Scheible, WR. (2009). Members of the *LBD* family of transcription factors repress anthocyanin synthesis and affect additional nitrogen responses in *Arabidopsis*. *Plant Cell,* 21(11), 3567–3584.

Sakamoto, T., et al. (2006). Erect leaves caused brassinosteroid deficiency increase biomass production and grain yield in rice. *Nat Biotechnol*, 24, 105-109.

Satoh-Nagasawa, N., Nagasawa, N., Malcomber, S., Sakai, H., & Jackson, D. (2006). A trehalose metabolic enzyme controls inflorescence architecture in maize. *Nature, 441*(7090), 227-230.

Schmid, M., Davison, T.S., Henz, S.R., Pape, U.J., Demar, M., Vingron, M., Scholkopf, B., Weigel, D., & Lohmann, J. (2005). A gene expression map of *Arabidopsis* development. *Nat Genet*, 37, 501-506.

Semiarti, E., Ueno, Y., Tsukaya, H., Iwakawa, H., Machida, C., & Machida, Y. (2001). The *ASYMMETRIC LEAVES2* gene of *Arabidopsis thaliana* regulates formation of a symmetric lamina, establishment of venation and repression of meristem-related homeobox genes in leaves. *Development,* 128, 1771–1783.

Sessions, A., et al. (2002). A high-throughput *Arabidopsis* reverse genetics system.

*Plant Cell,* 14(12), 2985-2994.

Shuai, B., Reynaga-Peña, C G., & Springer, P.S. (2002). The *LATERAL ORGAN BOUNDARIES* gene defines a novel, plant-specific gene family. *Plant Physiol, 129*(2), 747-761.

Smeekens, S., Ma, J., Hanson, J., & Rolland, F. (2010). Sugar signals and molecular networks controlling plant growth. *Curr Opin Plant Biol*, 13(3), 274-279.

Soyano, T., Thitamadee, S., Machida, Y., & Chua, N. (2008). *ASYMMETRIC LEAVES2-LIKE19/LATERAL ORGAN BOUNDARIES DOMAIN30* and *ASL20/LBD18* regulate tracheary element differentiation in *Arabidopsis*. *Plant Cell*, 20(12), 3359-3373.

Szymkowiak, E., & Sussex, I. (1996). What chimeras can tell us about plant development. *Ann Rev Plant Phyiols Plant Mol Biol*, 47, 351-376.

Takada, S., Hibara, K., Ishida, T., & Tasaka, M. (2001). The *CUP-SHAPED COTYLEDON1* gene of *Arabidopsis* regulates shoot apical meristem formation. *Development, 128*(7), 1127-1135.

Taramino, G., Sauer, M., Stauffer, J. L., Multani, D., Niu, X., Sakai, H., & Hochholdinger, F. (2007). The maize (*Zea mays* L.) *RTCS* gene encodes a LOB domain protein that is a key regulator of embryonic seminal and post-embryonic shoot-borne root initiation. *Plant J, 50*(4), 649-659.

Tian, F., et al. (2011). Genome-wide association study of leaf architecture in the maize nested associated mapping population. *Nature Genetics*, 43, 159-162.

Vollbrecht, E., Springer, P.S., Goh, L., Buckler IV, E.S., & Martienssen, R. (2005). Architecture of floral branch systems in maize and related grasses. *Nature,* 436 1119–1126.

Vroemen, C.W., Mordhorst, A.P., Albrecht, C., Kwaaitaal, M. A. C. J., & de Vries, S. C. (2003). The *CUP-SHAPED COTYLEDON3* gene is required for boundary and shoot meristem formation in *Arabidopsis*. *Plant Cell, 15*(7), 1563-1577.

Wahl, V., et al. (2013). Regulation of flowering by trehalose-6-phosphate signaling in *Arabidopsis thaliana*. *Science, 339*(6120), 704-707.

Wang, X., Zhang, S., Su, L., Liu, X., & Hao, Y. (2013). A genome-wide analysis of the LBD (LATERAL ORGAN BOUNDARIES Domain) gene family in *Malus*

*domestica with* a functional characterization of *MdLBD11*. *PLoS ONE, 8*(2), e57044.

Wingler, A. (2002). The function of trehalose biosynthesis in plants. *Phytochemistry, 60*(5), 437-440.

Winter, D., Vinegar, B., Nahal, H., Ammar, R., Wilson, G., & Provart, N. (2007). An "Electronic Fluorescent Pictograph" browser for exploring and analyzing large-scale biological data sets. *PLoS ONE*, 2(8), 718.

Yadav, R. K., Girke, T., Pasala, S., Xie, M., & Reddy, G. V. (2009). Gene expression map of the *Arabidopsis* shoot apical meristem stem cell niche. *Proc Natl Acad Sci USA, 106*(12), 4941-4946.

Yang, Y., Yu, X., & Wu, P. (2006). Comparison and evolution analysis of two rice subspecies *LATERAL ORGAN BOUNDARIES* domain gene family and their evolutionary characterization from *Arabidopsis*. *Mol Phylogenet Evol, 39*(1), 248-262.

Zhou, C., Han, L., Fu, C., Chai, M., Zhang, W., Li, G., Tang, Y., & Wang, Z. (2012). Identification and characterization of *petiolule-like pulvinus* mutants with abolished nyctinastic leaf movement in the model legume *Medicago truncatula. New Phytol*, 196(1), 92-100.

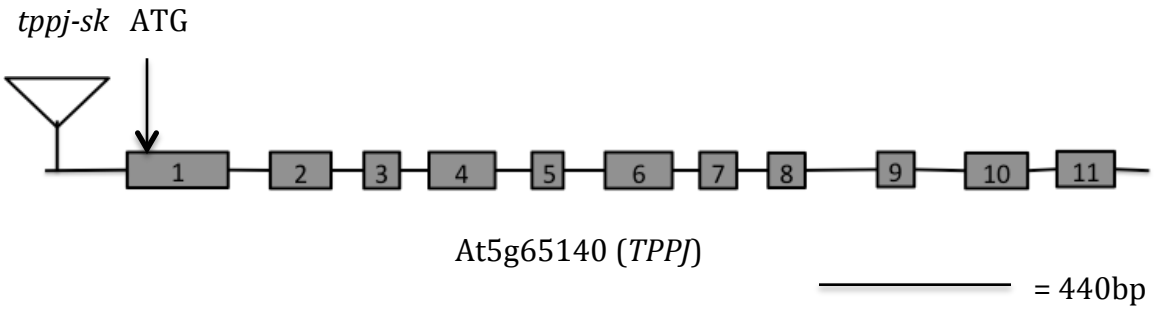


FIGURE 1 STRUCTURE OF THE *TPPJ-SK* T-DNA ALLELE (sk476)
Schematic showing the T-DNA insertion site of the *tppj-sk* mutant. Boxes represent exons and lines represent introns. The T-DNA insertion is located 300 bp upstream of the translation start site of *TPPJ* (At5g65140). Full length genomic sequence totals 2,635 bp.

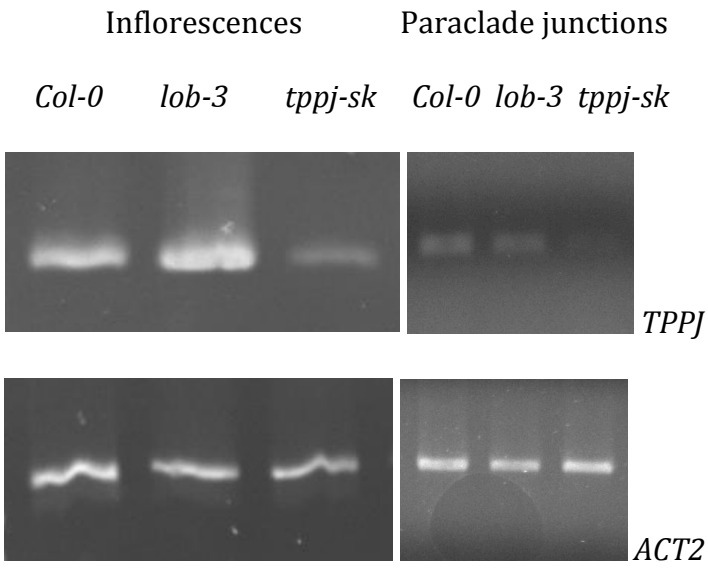


FIGURE 2 *TPPJ* TRANSCRIPT LEVELS IN DISSECTED INFLORESCENCES AND PARACLADE JUNCTIONS

RT-PCR analysis of *TPPJ* transcript levels. RNA was isolated from pools of inflorescences and paraclade junctions of wild-type *Col-0*, *lob-3* and *tppj-sk* plants. RT-PCR products were detected after 30 cycles of amplification for *TPPJ* transcripts. The lower panel shows RT-PCR using primers to the *ACT2* gene as a loading control (25 cycles of amplification).

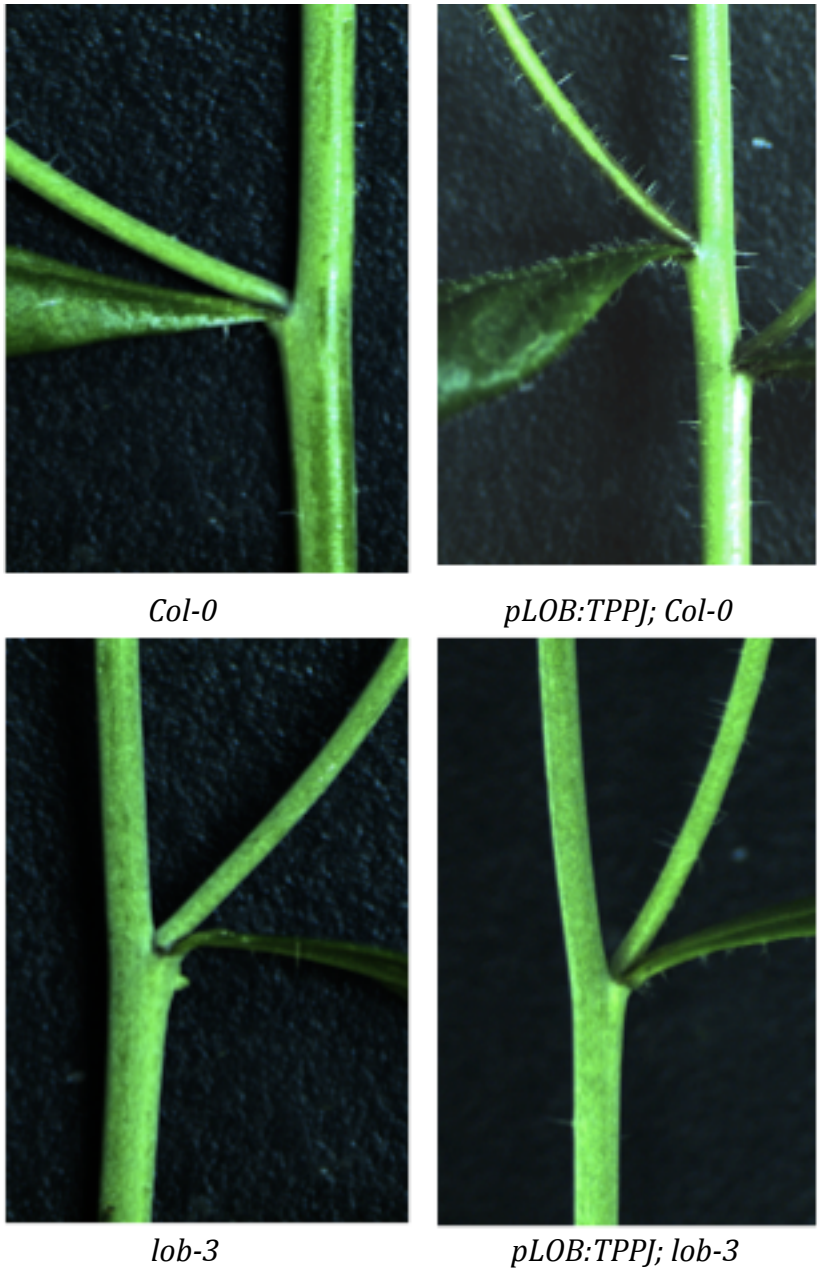


FIGURE 3 EXPRESSION OF *TPPJ* UNDER THE *LOB* PROMOTER SUPRESSES FUSION IN THE *lob* MUTANT

Phenotype of paraclade junction between main stem, axillary stem and cauline leaf in *Col-0, pLOB:TPPJ* in *Col-0*, *lob-3* and *pLOB:TPPJ* in *lob-3* plants. No organ fusion was detected in *Col-0*, *pLOB:TPPJ Col-0* and *pLOB:TPPJ lob-3* plants. Fusion of the axillary stem and cauline leaf are present in *lob-3* plants.

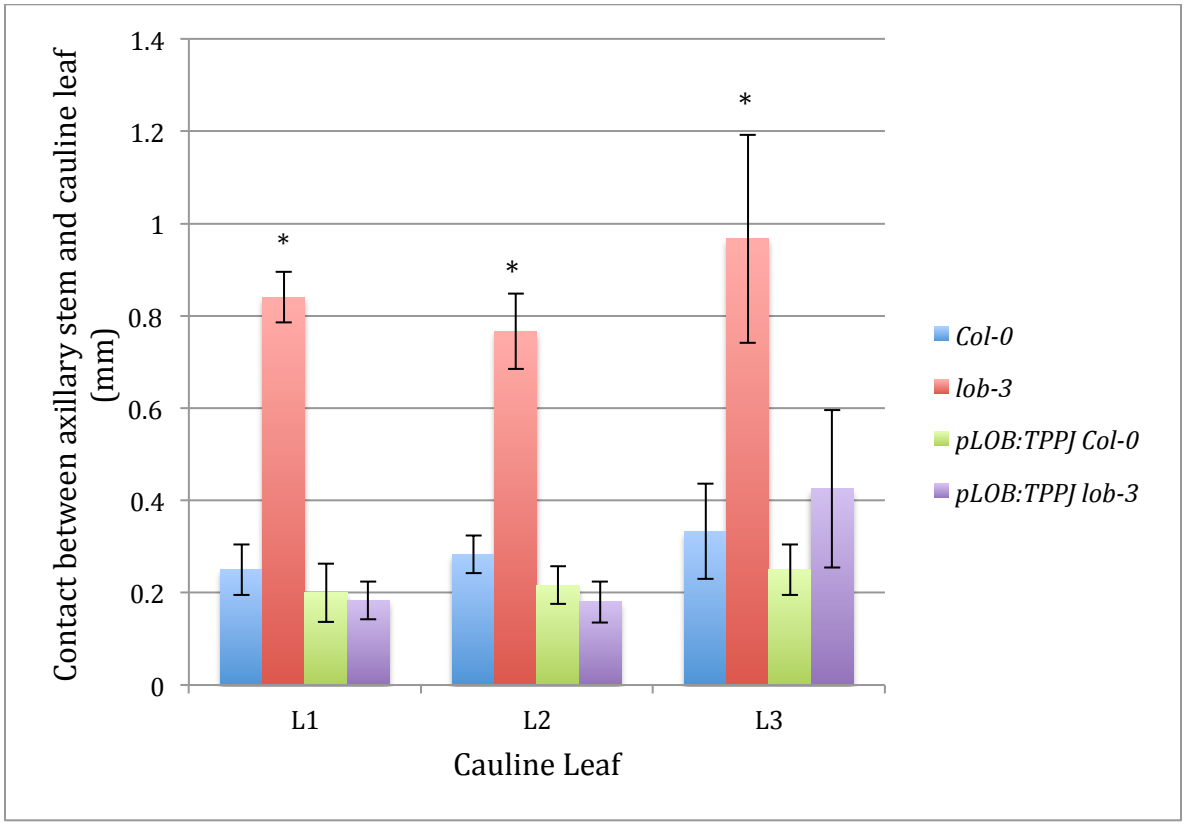


FIGURE 4 *pLOB:TPPJ* RESCUES *LOB-3* FUSION PHENOTYPE
Length of fusion between axillary stem and cauline leaf in *Col-0, pLOB:TPPJ* in *Col-0*, *lob-3* and *pLOB:TPPJ* in *lob-3* plants. L1 corresponds to lowest cauline leaf axil on the main stem. Standard deviations are indicated by error bars. n represents number of plants measured for each genotype. $n \geq 6$. n varies for each cauline leaf because not all plants have the same number of cauline leaves. Asterisk represents p-value < .05 (Student's T-Test in MS Excel).

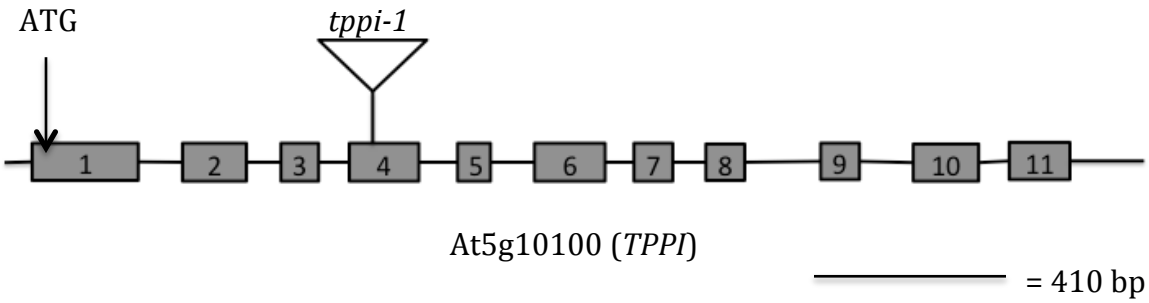


FIGURE 5 STRUCTURE OF THE *TPPI-1* T-DNA ALLELE (SAIL_354_D09)
Schematic showing the T-DNA insertion site of the *tppi-1* mutant. Boxes represent exons and lines represent introns. The T-DNA insertion is located in the 4$^{th}$ exon of *TPPI* (At5g10100). Full length genomic sequence totals 2,466 bp.

*Col-0*

*tppi-1*

*TPPI/TPPI*

*tppi-1*

FIGURE 6 PRESENCE OF DECURRENT STRAND IN *TPPI*-1 MUTANTS
Phenotype of paraclade junction between main stem, axillary stem and cauline leaf in *Col-0*, *tppi-1* and *TPPI/TPPI* plants. No organ fusion was detected in *Col-0* and most *TPPI/TPPI* plants. Fusion of the main stem and cauline leaf are present in *tppi-1* plants.

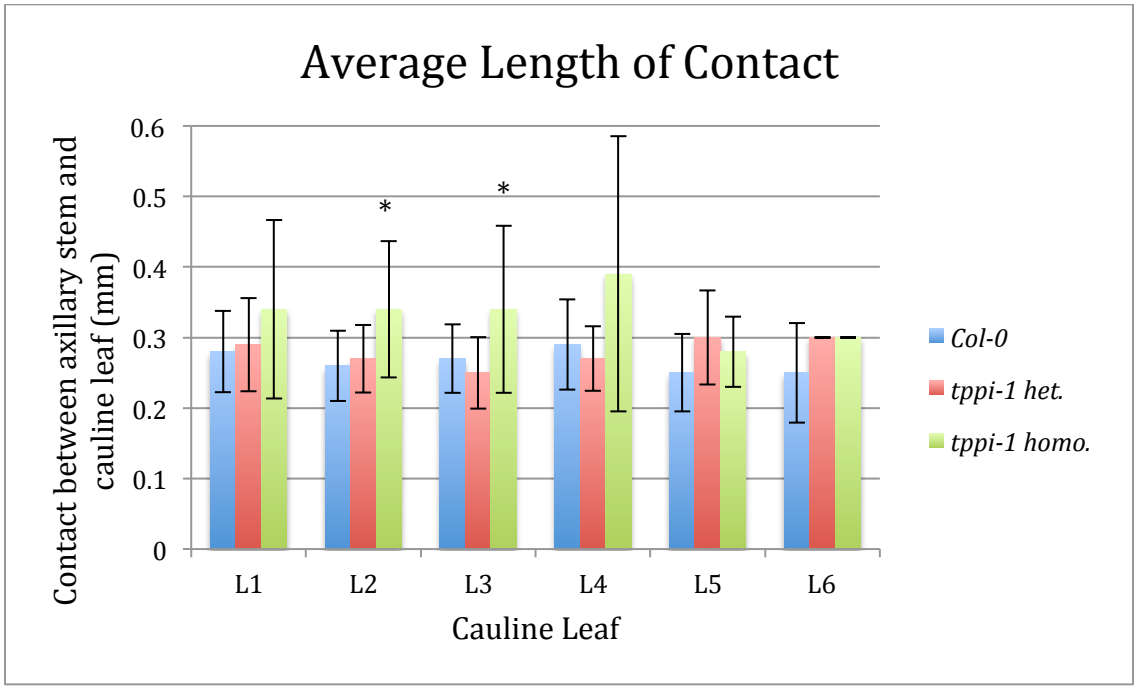


FIGURE 7 LENGTH OF CONTACT BETWEEN AXILLARY STEM AND CAULINE LEAF IS SIMILAR BETWEEEN t*ppi-1* MUTANTS AND *TPPI/TPPI*

Length of contact between axillary stem and cauline leaf in *TPPI/TPPI, tppi-1* heterozygous and *tppi-1* homozygous plants. L1 corresponds to lowest cauline leaf axil on the main stem. Standard deviations are indicated by error bars. n represents number of plants measured for each genotype. $n \geq 10$. n varies for each cauline leaf because not all plants have the same number of cauline leaves. Asterisk represents p-value < .05 (Student's T-Test in MS Excel).

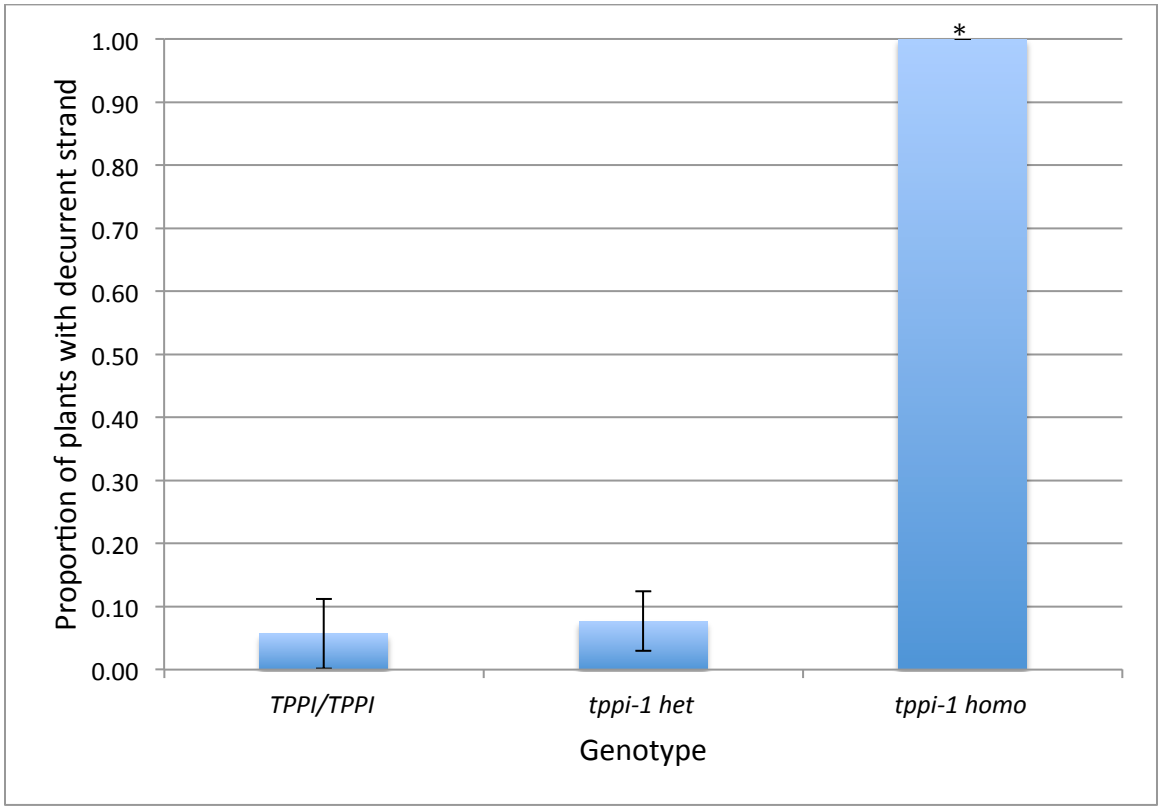


FIGURE 8 DECURRENT STRANDS OCCUR MOST FREQUENTLY IN *tppi-1* MUTANTS COMPARED TO TPPI/TPPI

Proportion of plants with decurrent strand present on main or axillary stem. Graph represents average of three biological replicates. Standard deviations are indicated by error bars. n represents number of plants measured for each genotype. $n \geq 10$. Asterisk represents p-value < .05 (Student's T-Test in MS Excel).

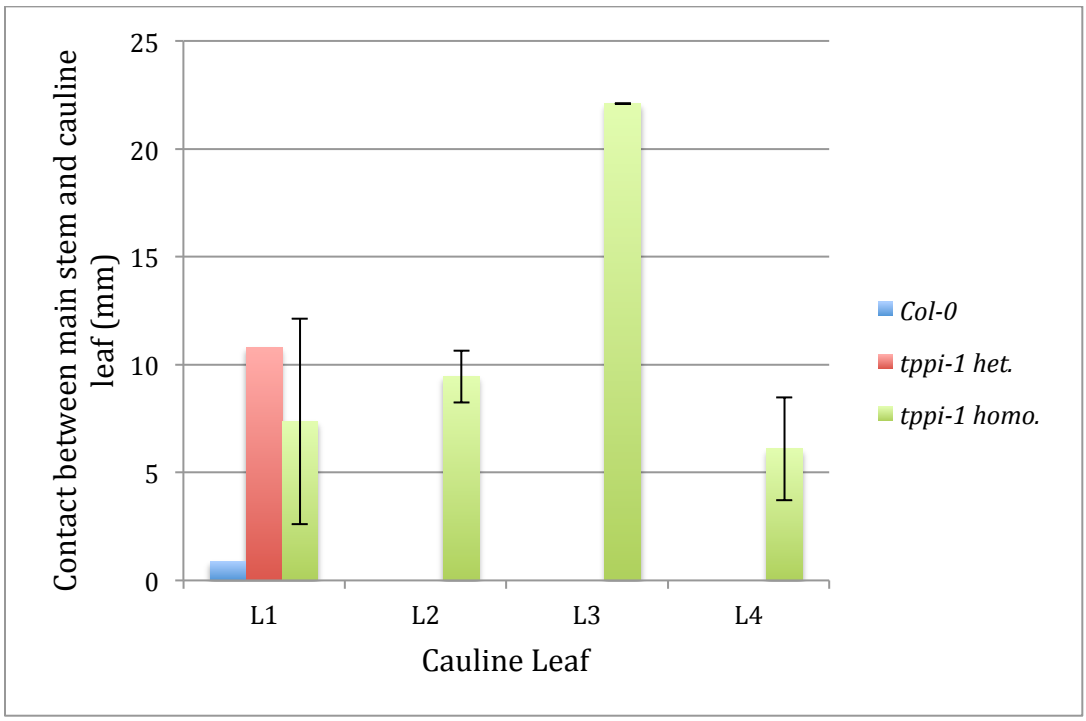


FIGURE 9 LENGTH OF DECURRENT STRANDS IS INCREASED IN t*ppi-1* MUTANTS COMPARED TO *TPPI/TPPI*

Length of fusion between main stem and cauline leaf in *TPPI/TPPI, tppi-1* heterozygous and *tppi-1* homozygous plants. L1 corresponds to lowest cauline leaf axil on the main stem. Standard deviations are indicated by error bars. $n \geq 10$. n varies for each cauline leaf because not all plants had the same number of cauline leaves.

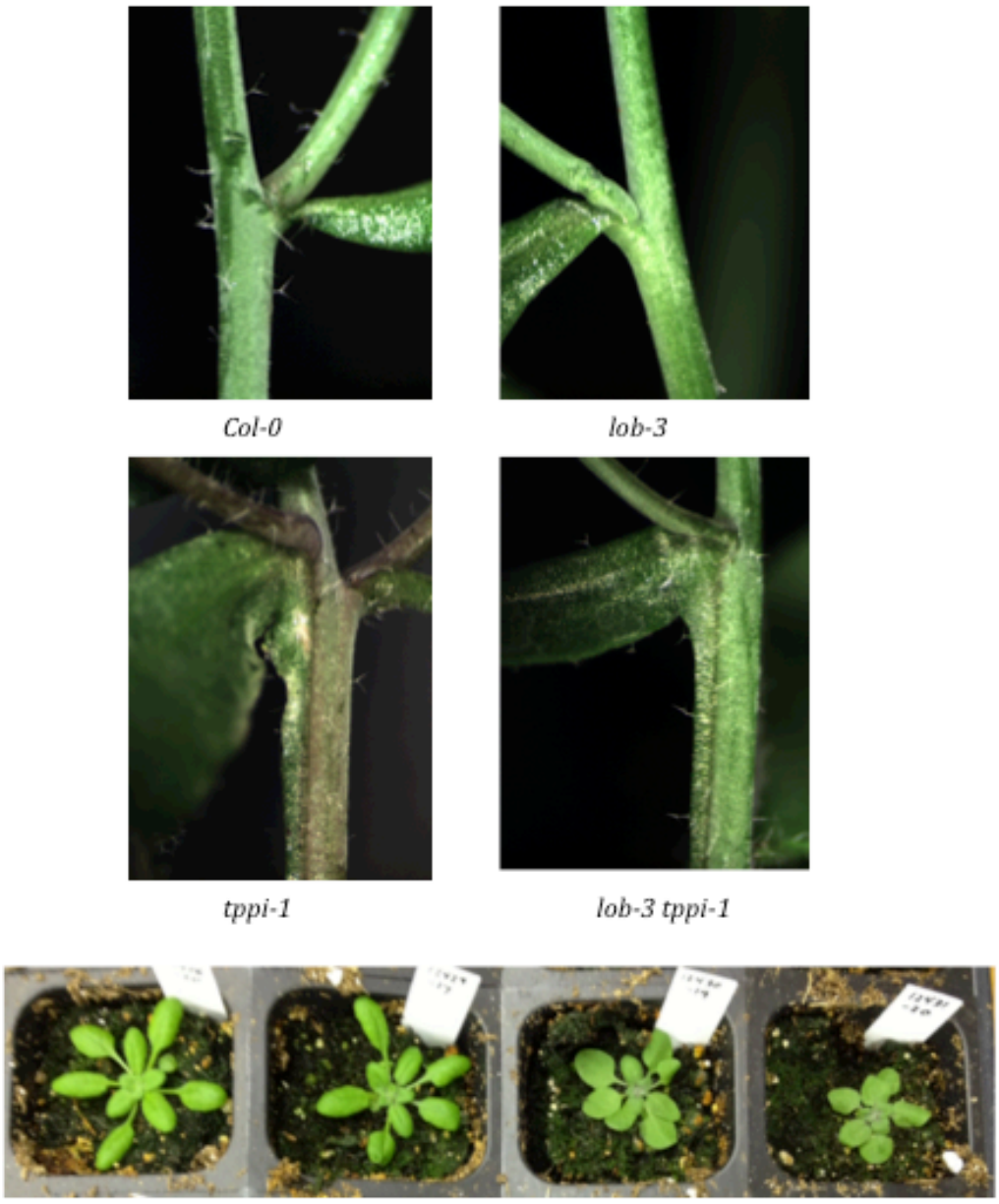


FIGURE 10 DECURRENT STRAND AND ROUND ROSETTE LEAVES PRESENT IN *tppi-1* and *lob-3 tppi-1* MUTANTS
Phenotype of paraclade junction between main stem, axillary stem and cauline leaf in *LOB/LOB TPPI/TPPI*, *lob-3*, *tppi-1* and *lob-3 tppi-1* plants. Fusion of the axillary stem and cauline leaf are present in *lob-3* and *lob-3 tppi-1* plants. Fusion of the main stem and cauline leaf are present in *tppi-1* and *lob-3 tppi-1* plants. Bottom picture shows round leaf phenotype present in *tppi-1* and *lob-3 tppi-1* plants.

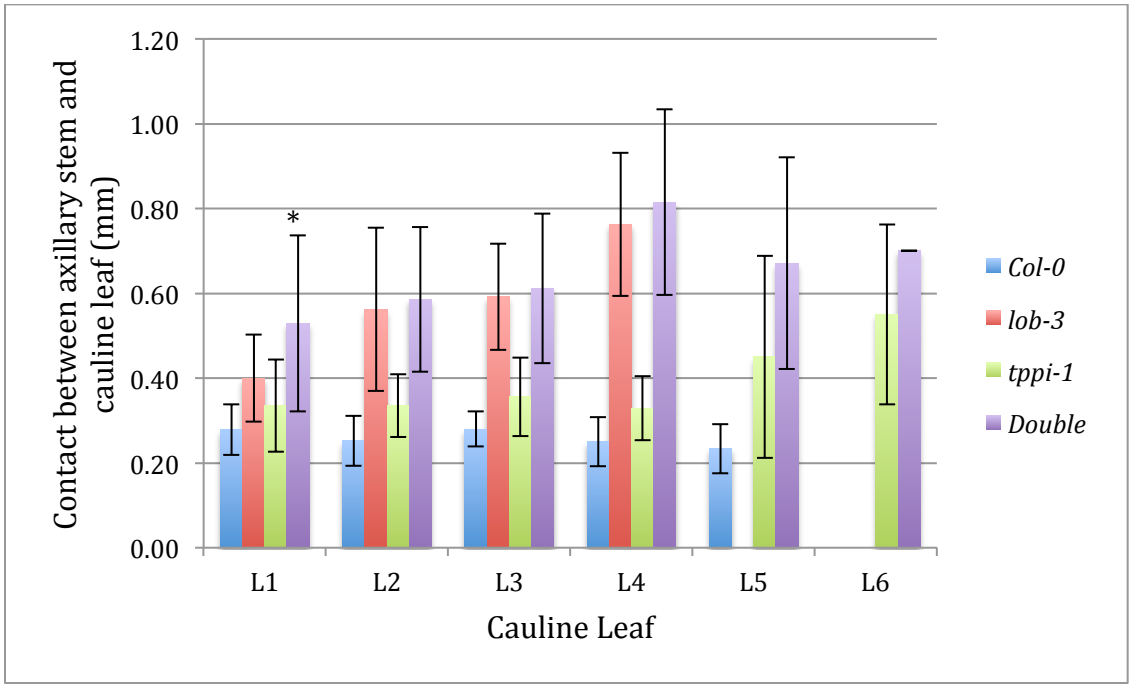


FIGURE 11 LENGTH OF CONTACT BETWEEN AXILLARY STEM AND CAULINE LEAF IN *lob-3* and *lob-3 tppi-1* MUTANTS

Length of fusion between axillary stem and cauline leaf in 23 *LOB/LOB TPPI/TPPI*, 16 *lob-3*, 20 *tppi-1* and 21 *lob-3 tppi-1* (double) plants. At L1, the double mutants are significantly different from *lob-3* plants. L1 corresponds to lowest cauline leaf axil on the main stem. Standard deviations are indicated by error bars. n represents number of plants measured for each genotype. $n \geq 16$. n varies for each cauline leaf because not all plants have the same number of cauline leaves. Asterisk represents p-value < .05 (Student's T-Test in MS Excel).

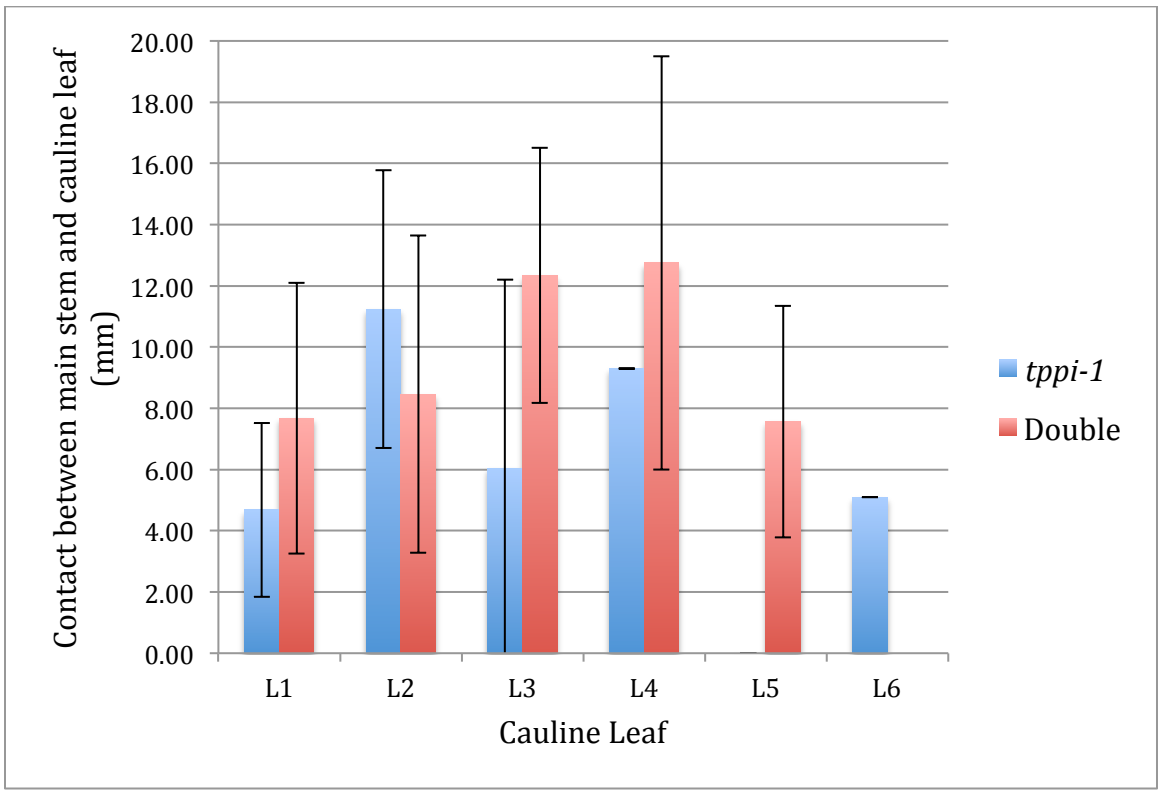


FIGURE 12 LENGTH OF DECURRENT STRANDS IN *tppi-1* and *lob-3 tppi-1* MUTANTS
Length of fusion between main stem and cauline leaf in *tppi-1* and *lob-3 tppi-1* double-mutant plants. L1 corresponds to lowest cauline leaf axil on the main stem. Standard deviations are indicated by error bars. n varies for each cauline leaf because not all plants have the same number of cauline leaves.

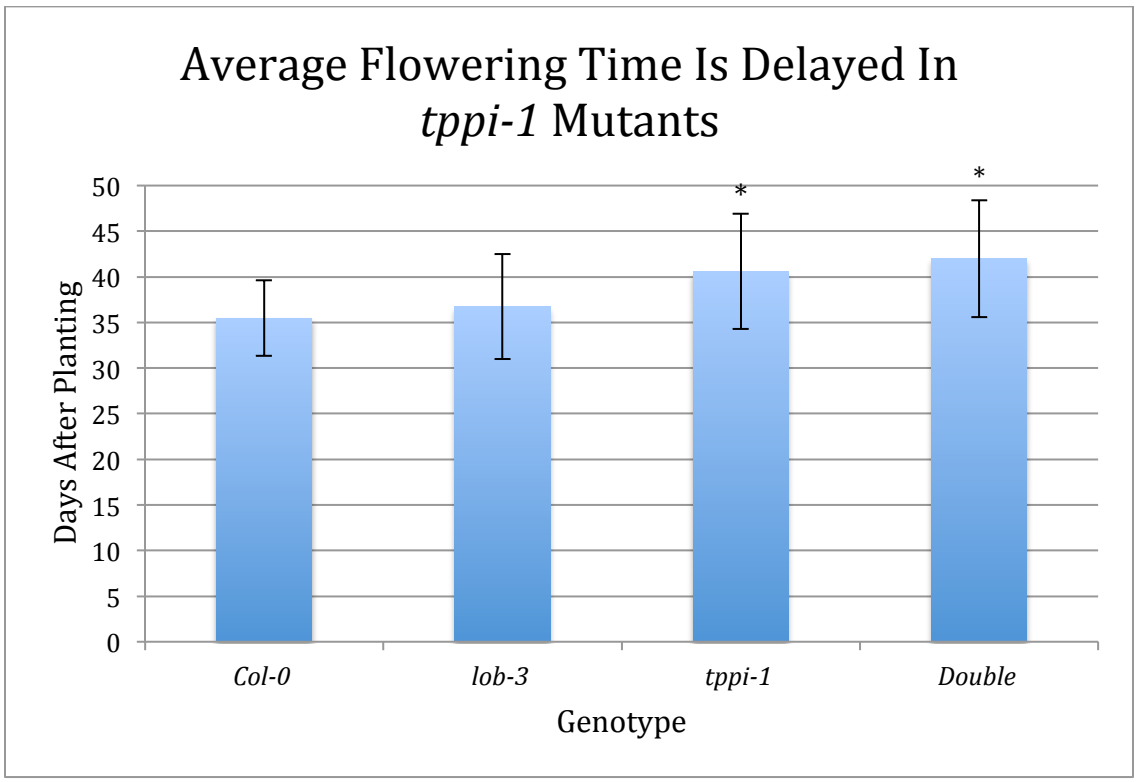


FIGURE 13 *TPPI-1* MUTANTS SHOW DELAYED FLOWERING
Average flowering time in *LOB/LOB TPPI/TPPI*, *lob-3*, *tppi-1* and *lob-3 tppi-1* double-mutant plants. Standard deviations are indicated by error bars. n represents number of plants measured for each genotype. $n \geq 16$. Asterisk represents p-value < .05 (Student's T-Test in MS Excel).

TABLE 1 LIST OF OLIGONUCLEOTIDE SEQUENCES

| Primer Name | Sequence 5' to 3' | Pupose |
|---|---|---|
| At5g65140F | CTCGGGGACACGTGGCCT | *TPPJ* Genotyping |
| pSKTAIL-L3 | ATACGACGGATCGTAATTTGTCG | *TPPJ* Genotyping |
| At5g65140F RT | CGTCGTATCAGACGCCAAGACCGGG | *TPPJ* RT-PCR |
| At5g65140R RT | CCACGATCGGAGAAAGAGTACCGT | *TPPJ* RT-PCR/*TPPJ* Genotyping |
| TPPJ F | CACCATGGTGAGCCAAAAC | *TPPJ* Cloning |
| TPPJ R | TTATTGCTGCATCTGTTTCCA | *TPPJ* Cloning |
| TPPI-1 520 INTRON FW | TTAATCTGTTTTGACTTGATCATATTTTG | *TPPI* Genotyping |
| TPPI-1 1101 INTRON RV | AATCAATACTCAACTCATATGTACGACAA | *TPPI* Genotyping |
| At5g10100F | GGAAGCTTCGAGAGGGAAACAAATCGT | *TPPI* Genotyping |
| LB3 | TAGCATCTGAATTTCATAACCAATCTCGATACAC | *TPPI* Genotyping |
| TPPI F RTPCR | GTGACAATATTCGAAATGCCAAT | *TPPI* RT-PCR |
| TPPI-R GW | CCTAATGGGGGTACGTTAAAGA | *TPPI* RT-PCR/*TPPI* Cloning |
| TPPI F | CACCATGTCAGCTAGTCAAAAC | *TPPI* Cloning |
| LOB-RKF | CCACACACAGTCCATGCATTA | *lob-3* Genotyping |
| LOB-RKR | GCGTCGTCATCAAACTCATA | *lob-3* Genotyping |
| LBa1 | TGGTTCACGTAGTGGGCCATCG | *lob-3* Genotyping |
| ET22-1 | TTCTTCGCCGGAAATGCA | *Et22* Genotyping |
| SET223' | GCTCTAGACTCACATGTTACCTCCTTGC | *Et22* Genotyping |
| DS3-4N | CCGTCCCGCAAGTTAAATATG | *Et22* Genotyping |
| ACT2-C | ACTCACCACCACGAACCAG | Loading control |
| ACT2-N | AAAATGGCCGATGGTGAGG | Loading control |
| Plob F2 | TCTAAACGAAACGTAGGAGT | Promoter *LOB* |
| pLOB-R | CTGCAGACGACGCCATTTGTTTTTCTT | Promoter *LOB* |
| MDC-8 | TTGGAAGCGAAATTCAAAGG | Promoter *LOB* |